Nucleic Acids Research, 1997, Vol. 25, No. 24 **4907–4914**

Electric field directed nucleic acid hybridization on microchips

Carl F. Edman, Daniel E. Raymond, David J. Wu, Eugene Tu, Ronald G. Sosnowski, William F. Butler, Michael Nerenberg and Michael J. Heller*

Nanogen, 10398 Pacific Center Court, San Diego, CA 92121, USA

Received September 11, 1997; Revised and Accepted November 3, 1997

ABSTRACT

Selection and adjustment of proper physical parameters enables rapid DNA transport, site selective concentration, and accelerated hybridization reactions to be carried out on active microelectronic arrays. These physical parameters include DC current, voltage, solution conductivity and buffer species. Generally, at any given current and voltage level, the transport or mobility of DNA is inversely proportional to electrolyte or buffer conductivity. However, only a subset of buffer species produce both rapid transport, site specific concentration and accelerated hybridization. These buffers include zwitterionic and low conductivity species such as: D- and L-histidine; 1- and 3-methylhistidines; carnosine; imidazole; pyridine; and collidine. In contrast, buffers such as glycine, β-alanine and γ-amino-butyric acid (GABA) produce rapid transport and site selective concentration but do not facilitate hybridization. Our results suggest that the ability of these buffers (histidine, etc.) to facilitate hybridization appears linked to their ability to provide electric field concentration of DNA; to buffer acidic conditions present at the anode; and in this process acquire a net positive charge which then shields or diminishes repulsion between the DNA strands, thus promoting hybridization.

INTRODUCTION

Microchip-based nucleic acid arrays now permit the rapid analysis of genetic information by hybridization (1–6). Many of these devices take advantage of sophisticated silicon manufacturing processes developed by the semiconductor industry over the last 40 years. In these devices, many parallel hybridizations may occur simultaneously on immobilized capture probes. Stringency and rate of hybridization is generally controlled by temperature and salt concentration of the solutions and washes. Such 'passive' micro-array approaches have several limitations. First, as all nucleic acids are exposed to the same conditions simultaneously, capture probes must have similar melting temperatures to achieve similar levels of hybridization stringency. This places limitations on the length, GC content and secondary structure of the capture probes. Second, as the rate of hybridization is proportional to the initial concentration of the interrogated solution, high concentrations are required to achieve rapid hybridization. Third, because of difficulties controlling hybridization conditions, single base discrimination is generally restricted to oligomers of 20 bases or less with centrally placed differences (1).

In an attempt to circumvent these limitations, we have developed microchip-based hybridization arrays that utilize electric fields as an independent parameter to control DNA transport, enhance hybridization, and improve the stringency of nucleic acid interactions (7,8). We refer to these as 'active' microelectronic devices in that they exploit both microfabrication and microelectronic technology, and that they directly affect the hybridization reactions. In addition to salt, pH, temperature and chaotropic agents, the electric field strength allows another precisely controlled and continuously variable parameter for adjustment of hybridization interactions.

Electronic addressing and/or hybridization is carried out by selective application of a DC positive bias to the individual microelectrodes beneath the selected test sites. This causes rapid transport and concentration of negatively charged nucleic acid molecules over selected locations on the microelectronic array. The nucleic acid (DNA, RNA, polynucleotides, oligonucleotides, etc.) may then be immobilized by direct attachment to the permeation layer overlying the micro-electrode or by hybridization to a previously addressed and attached nucleic acid. This rapid concentration leads to a dramatic reduction in time for hybridization when compared to passive hybridization techniques. Thus, hybridization occurs in seconds rather than hours. Reversal of the electric potential then allows rapid removal of unhybridized molecules, as well as continuous adjustment of stringency.

We have experimentally determined several factors that facilitate this process. A crucial role is played by the ion-permeable layer which overlies the micro-electrodes. This layer allows attachment of nucleic acids. Ultimately, this enables single-stranded nucleic acids to be 'electronically targeted' above these micro-electrodes and hybridized to the anchored complementary oligonucleotides while being protected from the reactive environment present at the electrode surface. The structure of typical arrays and permeation layers has been described previously (7,8).

Another important consideration is the composition of the transport and hybridization buffers. To facilitate rapid movement of nucleic acids by free solution electrophoresis, we have utilized low conductivity buffers. To achieve low conductivity and preserve good buffering capacity, we have used zwitterions that have no net charge near neutral pH. These buffers typically possess conductivities less than 100 microSiemens per cm (μS/cm). Buffers commonly employed in molecular biology have conductivities a thousand-fold

*To whom correspondence should be addressed. Tel: +1 619 546 7700; Fax: +1 619 546 7718; Email: mheller@nanogen.com

greater, e.g. 6× sodium chloride/sodium citrate (SSC) (9). Many of these low conductivity and zwitterionic buffers with no net charge do not optimally shield nucleic acid phosphodiester backbone charges and, therefore, under passive conditions do not aid in hybridization. However, they do probably help to prevent self-annealing of denatured nucleic acids in the transport process. We have now discovered that some buffer species (histidine, etc.) do facilitate both transport and the accelerated hybridization of DNA at the micro-array test sites. We present herein our findings concerning the characteristics of the low conductivity and zwitterionic buffers which facilitate these processes.

MATERIALS AND METHODS

Reagents

Buffers and chemicals utilized were purchased from Sigma (St. Louis, MO), Aldrich, (Milwaukee, WI), ICN Biochemicals (Aurora, OH), Boehringer-Mannheim (Indianapolis, IN) or Calbiochem (San Diego, CA). Oligonucleotides were synthesized as before (8) or were purchased from Oligo Therapeutics (Wilsonville, OR). Peptide nucleic acid (PNA) oligonucleotide analogues were synthesized by PerSeptive Biosystems. Conjugation of functional groups and oligonucleotide purification has been described previously (8).

Microelectronic chips, permeation layer and instrumentation

These have been described previously (8). In brief, the 5580 series APEX chip used for these experiments consists of a 5 × 5 array of 80 μm circular microelectrodes with 200 μm microelectrodes at each corner of the array. Chips were mounted on a micromanipulator stage and the microelectrodes activated by a power supply and appropriately controlled relay switches. Fluorescent labeled oligonucleotides on the chip were visualized using oblique illumination with two 594 nm HeNe lasers and the images were quantified using either NIH Image or IPLab Spectrum software packages.

Accumulation and hybridization

Two biotinylated capture oligonucleotides, ATA5 and ATA4 (8) were electronically transported and localized at adjacent microelectrodes. The solution was removed and the chip washed three or four times in test buffer. Buffers employed in these studies are listed in Table 1 and were utilized at the listed pH values and concentrations presented. The L-isomers of amino acids were used, unless otherwise noted. The chip was equilibrated in test buffer for 5–10 min. Then fresh buffer containing 10 nM BODIPY-Texas Red labeled RCA5 (btrRCA5), an oligonucleotide complementary to ATA5 but not ATA4 (8) was applied. The 200 μm microelectrodes were employed as cathodes and one microelectrode within the array used as the corresponding anode. Accumulation was assessed by sourcing a 500 nA constant current to individual microelectrodes for 30 s and monitoring the accumulation of fluorescence at the positively-biased (anode) site in the microelectrode array. Signal arising from non-fluorescent sources (i.e., detector thermal noise, etc.) was subtracted. Experiments examining the effect of different currents upon signal accumulation were conducted in a similar fashion except that the applied current varied from 100 nA to 1 μA. Initial rates were calculated for the first 5 s of signal accumulation, during which linear fluorescence accumulation was observed in all buffers. For the comparison between conductivities of various buffers, data is presented as fold increase over initial fluorescence to account for chip-to-chip variation as well as laser illumination variations in signal levels. For other experiments, data is presented as attomol product versus time, after converting the observed fluorescence intensity to moles of labeled oligonucleotide. (Absolute calibration of the fluorescence signal intensity to the surface density of fluorophores was done by measuring fluorescence from 10–20 μm thin film solutions containing known concentrations of fluorescent labeled oligonucleotides layered over an unpatterned platinum surface.) Control experiments indicate that fluorescence measurements were unaffected by buffers and conditions employed.

Table 1. Buffer properties

Buffer	Concentration	pKa[a]	pI	pH[b]	Conductivity (μS/cm)
glycine	50 mM	2.34, 9.60	5.97	6.01	2.5 ± 0.2
glycine	250 mM	2.34, 9.60	5.97	6.11	7.8 ± 0.5
β-alanine	50 mM	3.60, 10.19	6.90	6.71	3.6 ± 0.6
GABA	50 mM	4.03, 10.56	7.30	6.76	5.6 ± 0.6
cysteine	50 mM	1.71, 8.33, 10.78	5.02	5.08	9.0 ± 0.9
cysteine	250 mM	1.71, 8.33, 10.78	5.02	nd[d]	21.8 ± 4.4
3(τ)-methylhistidine	50 mM	1.70, 5.87, 9.16[c]	7.52	7.44	39.4 ± 0.4
D-histidine	50 mM	1.78, 5.97, 8.97	7.47	7.70	57.1 ± 0.3
L-histidine	50 mM	1.78, 5.97, 8.97	7.47	7.65	60.1 ± 0.1
carnosine	50 mM	2.64, 6.83, 9.51	8.17	8.07	74.5 ± 5.5
1(π)-methylhistidine	50 mM	1.64, 6.46, 8.61[c]	7.54	7.59	117 ± 2.8
pyridine	50 mM	5.19	–	8.17	5.0 ± 0.8
imidazole	50 mM	6.99	–	9.08	17.6 ± 1.6
collidine	50 mM	6.69	–	9.85	33.0 ± 0.9

[a]Values obtained from Budavari, S. (1989) *The Merck Index*, 11th Ed., Merck & Co., Inc., Rahway, NJ, unless otherwise noted.
[b]pH of buffer solution measured in water at room temperature.
[c]Remelli, M., Munerato, C. and Pulidori, F. (1994) *J. Chem. Soc. Dalton Trans.*, 2049–2056.
[d]nd, not determined.

Following accumulation at one microelectrode location, the buffer was removed and fresh buffer containing btrRCA5 applied. An adjacent microelectrode was then sourced in a similar fashion. Upon completion, the buffer was removed and the chip washed between five and seven times with test buffer without btrRCA5. The pair of previously targeted microelectrodes were then illuminated and the fluorescence present at each site quantified. Control experiments utilized a bodipy-Texas Red labeled oligonucleotide complementary to ATA4 to verify the integrity and concentration of the ATA4 capture oligonucleotide. Percent hybridization efficiency was calculated as follows: (complementary oligonucleotide signal – non-complementary signal)/(signal present immediately prior to the end of the applied current) × 100.

Buffer conductivity and pH measurements

The conductivities of test buffer solutions utilized for transport and hybridization were measured at room temperature using an Accumet 1.0 cm^{-1} glass conductivity cell connected to an Accumet Model 50 pH/Ion/Conductivity meter (Fisher Scientific). Buffer pH values were obtained using an Accu-pHast variable temperature combination electrode and the same model meter.

Micro-pH measurements

Antimony electrodes were fabricated using methods described elsewhere (10) with the following minor modifications. Theta glass (World Precision Instruments, Sarasota, Florida) was used to obtain a double barrel type electrode, plus all capillaries were hand pulled with a final tip diameter estimated to be 75 µm. The potential of the antimony electrode was measured relative to a Ag/AgCl reference electrode using the pH meter employed above. Calibration of the antimony electrode yielded a slope of 57 mV/pH, a value in good agreement with other literature values (10–13). While viewed through a microscope, the antimony electrode was brought down to the surface of an agarose coated chip using a motorized X-Y-Z micromanipulator until the electrode was observed to bend. Afterwards the electrode was raised to a height just above the observed deflection point. The distance from the antimony electrode to the chip surface was estimated to be 7 µm. The antimony electrode tip was then positioned over individual microelectrode wells at an oblique angle so as to minimize diffusion effects (10). The pH readings were obtained using either 200 or 500 nA constant current in either 50 mM KCl, 50 mM histidine, 50 mM imidazole or 50 mM γ-amino-butyric acid (GABA).

Passive hybridization versus electric field hybridization

ATA5 was electrically targeted to the first four columns of the microarray on streptavidin/agarose coated chips prepared as above, and ATA4 was targeted to the remaining column. For passive hybridization, either 5.0 or 0.5 nM btrRCA5 in 5× SSC (1× = 0.15 M NaCl, 15 mM sodium citrate, pH 7.0) was applied for 1 min, then the chips were washed six times in buffer and imaged. For the 3 min timepoint, fresh buffer containing btrRCA5 was applied and incubated for an additional 2 min to achieve 3 min cumulative incubation time. This approach was repeated for the remaining time points. A similar experiment was performed using 5 nM btrRCA5 in 50 mM histidine. For electric field hybridization, either 5.0 or 0.5 nM btrRCA5 in 50 mM histidine was applied. Five sites, four with ATA5 previously attached and one with ATA4, were electronically targeted using 3.1 V total (~500 nA/site). Following application of the current for the desired time period, the chip was washed six times in histidine and imaged. Other data points were obtained in a similar fashion by targeting fresh solutions of btrRCA5 in histidine to previously untargeted sites for the indicated times. In both passive and electric field mediated hybridization, the background signal present at the ATA4 sites was subtracted from the signal present at ATA5 sites.

Comparison of hybridization of phosphodiester-linked oligonucleotides to PNA analogues

Thirty µM biotinylated oligodeoxyribonucleotides or PNA analogues were microdeposited upon individual sites of a streptavidin/agarose coated microarray in 10% glycerol, 25 mM NaCl, 25 mM sodium phosphate, pH 7.4, using an Eppendorf Micromanipulator 5171 and Transjector 5246. Following a 30 min incubation, the chip was rinsed with water. Sequences are as follows:

DNA1: biotin-d(CACCTGCTTTGATAGCTG)
PNA1: biotin-O-O-CACCTGCTTTGATAGCTG, O = ethylene glycol linker
DNA2: biotin-d(GATGAGCAGTTCTACGTGG)
PNA2: biotin-O-O-TGTACGTCACAACTA
Reporter DNA: btr-d(CAGCTATCAAAGCAGGTG), btr = BODIPY-Texas Red

DNA1 and PNA1 are complementary to reporter DNA whereas DNA2 and PNA2 serve as controls to evaluate non-specific hybridization. Electronic hybridization was performed with 5 µl of DNA reporter probe in 50 mM GABA or 50 mM histidine. The chip was electronically activated for 10 or 30 s at 200 nA or 30 s at 500 nA. Following each electronic hybridization, the chip was rinsed several times with the same buffer. After the final electronic hybridization, the chip was washed in a mixture of 0.2× STE (20 mM NaCl, 2 mM Tris–HCl, pH 8.0, 0.2 mM EDTA, pH 8.0) and 0.1% sodium dodecyl sulfate, then 0.2× STE alone and a final image taken. Hybridization efficiency was calculated as above.

Passive hybridization at different pHs

Biotinylated ATA5 and ATA4 were electronically targeted to adjacent sites upon streptavidin/agarose coated microarrays. Buffer consisting of 100 nM btrRCA5 in 50 mM histidine at its pI value (pH ≈ 7.5) or adjusted to either pH 6.0, 5.0, 4.0 or 3.0 with HCl, was added to each chip and allowed to react for 10 min. A parallel hybridization was done in 6× SSC. After this hybridization period, the chips were washed in 0.2× STE, 0.1% sodium dodecyl sulfate, as above and the remaining fluorescence at each site quantitated. Fluorescence values present at ATA4 sites were subtracted from adjacent ATA5 sites and the remaining fluorescence converted to attomol btrRCA5 specifically hybridized. Additional experiments repeated this methodology and also examined buffer adjusted with concentrated acetic acid (at the pI and at pH 6 and 5). Similar results were observed.

RESULTS

Effect of buffer composition on oligonucleotide transport

To promote hybridization of complementary nucleic acid in a dilute solution, the sample must be concentrated over the capture

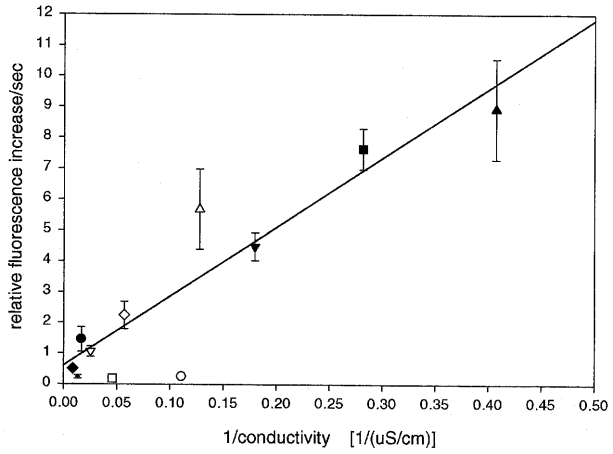

Figure 1. Oligonucleotide accumulation in different conductivity buffers using constant current. Fluorescent labeled oliogonucleotide, btrRCA5, added in various test buffers, was analyzed at a constant current of 500 nA. The accumulation of fluorescent signal at the activated anode was monitored. The initial rate of fluorescence increase was calculated based upon the starting fluorescence, as described in Materials and Methods. Test buffers: ● = 50 mM L-histidine; ○ = 50 mM cysteine; + = 50 mM carnosine; ■ = 50 mM β-alanine; □ = 250 mM cysteine; ▲ = 50 mM glycine; Δ = 250 mM glycine; ▼ = 50 mM GABA; ∇ = 50 mM 3-methylhistidine; ◆ = 50 mM 1-methylhistidine; ◇ = 50 mM imidazole. Data are presented as mean ± SD (n ≥ 4). The straight line indicates a least squares fit to all data.

sequence. This causes a local increase in the C_0t value, increasing the rate of hybridization by mass action. Under constant current conditions, charge is transported by all ionic species in the solution and thus buffer conductance determines the proportion of the current carried by the oligonucleotide. To measure this, fluorescent labeled reporter oligonucleotides were electronically targeted to locations where either complementary or non-complementary oligonucleotides had previously been attached. Accumulation of fluorescent signal over time in response to the applied current was then assessed for several different buffers (Table 1). We noted that accumulation eventually reaches a plateau. Therefore, to accurately measure the effects of conductivity, we have measured the initial rate of accumulation. Figure 1 displays analysis of a representative selection of buffers. The initial increase in fluorescent signal is compared to the inverse of buffer conductivity (i.e., solution resistance). This plot shows a roughly linear relationship between the solution resistance and the accumulation of signal. The more conductive the solution, the slower the rate of oligonucleotide accumulation.

Interestingly, the rate of accumulation in cysteine (open circle and open square in Fig. 1) was lower than would be expected based upon initial conductivity. One possible explanation is that the sulfhydryl group of cysteine is electrochemically reactive at voltages lower than that required for the hydrolysis of water (14) and generates additional reactive ions or molecules. Therefore, factors other than the initial solution conductivity may govern microscale electrophoretic transport and hybridization properties of buffers such as cysteine.

As mentioned above, we also noted a progressive slowing of fluorescence accumulation, the rate of which differed between buffer solutions. At a constant current, a gradient of ionic strength builds from the electrode into the bulk solution over time (15,16). This results in an increase in the conductivity of the solution immediately above the electrode. This increase in conductivity results in lower mobility or a decreasing rate of DNA accumulation. In addition, as DNA accumulates above the electrode, diffusion increasingly opposes the electric field-mediated transport of DNA, also slowing the overall rate of accumulation. Eventually, a steady state might be reached where the diffusion rate equals the electric field transport resulting in no further net accumulation of the oligonucleotides (16). In addition, the mobility of the oligonucleotides decreases as they encounter regions where the electrochemically mediated decrease in pH (see below) matches the pI of the oligonucleotide. Finally, signal could be lost by the electrochemical quenching of the fluorescent signal later in the reaction.

If the nucleic acid alone carried the current, migration of the charged oligonucleotides would be predicted to be proportional to the applied current. However, analysis of Figure 2 demonstrates

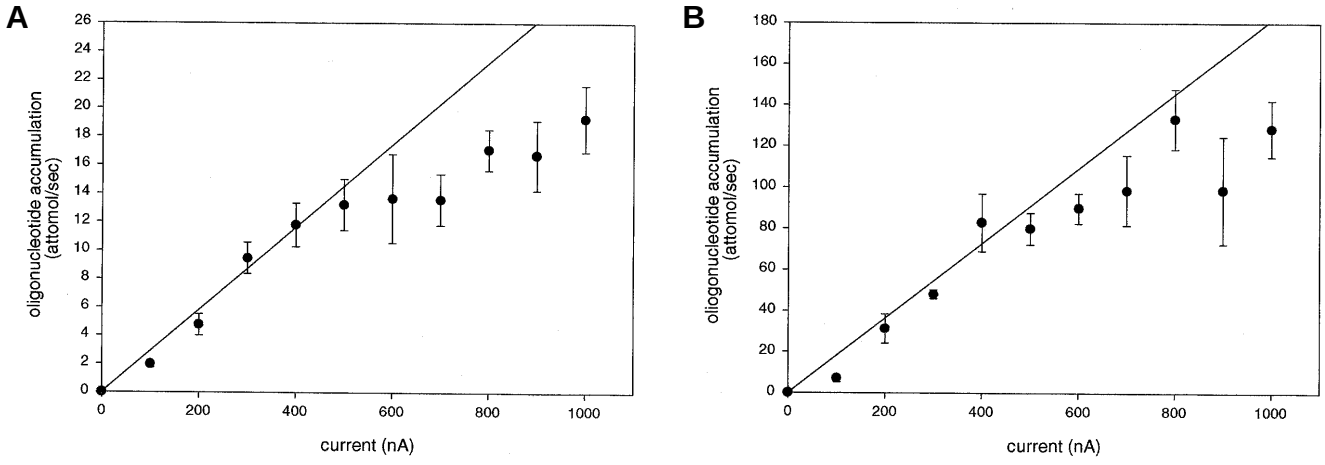

Figure 2. Effect of increasing current upon oligonucleotide accumulation. Buffer containing btrRCA5, 10 nM, was applied to test chips and individual microelectrode sites were activated using the indicated current levels for 30 s. Oligonucleotide accumulation at each microelectrode was monitored by fluorescence intensity and the initial rate of accumulation at each site calculated, as described in Materials and Methods. (**A**) Rate of oligonucleotide accumulation in 50 mM L-histidine. (**B**) Rate of oligonucleotide accumulation in 50 mM GABA. Data are presented as mean ± SEM (n = 4). In both panels, a linear extrapolation of the data from 0 to 400 nA is shown.

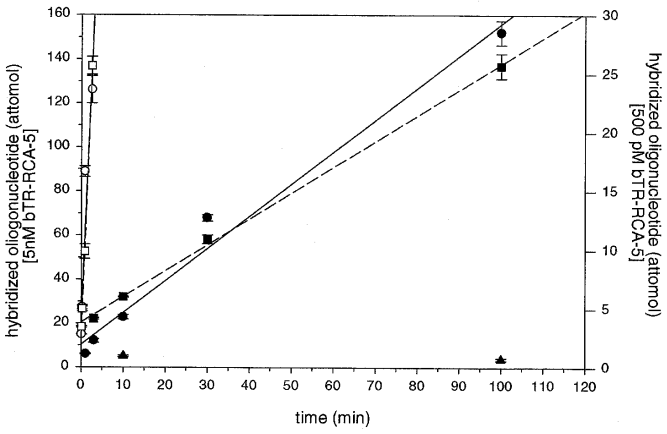

Figure 3. Comparison between passive hybridization and electronically-mediated hybridization. As described in Materials and Methods, capture oligonucleotides, either ATA5 or ATA4, were attached to various microelectrode sites upon an APEX chip microarray. btrRCA5, 5 nM (○) or 500 pM (□), was then introduced in 50 mM L-histidine and then electronically targeted to previously addressed pads at 3.1 V constant (~500 nA per targeted site). On other chips, capture oligonucleotides were addressed as above and then btrRCA5, either 5 nM in 5× SSC (●) or 50 mM L-histidine (▲) or 500 pM in 5× SSC (■), was added and allowed to passively hybridize. At the indicated time points, the reactions were stopped, the chips washed, and the fluorescence signal quantified. Solid lines indicate least squares fit to 5 nM data; dashed lines indicate least squares fit to 500 pM data; passive hybridization in histidine are presented as individual points. Data are presented as mean ± SEM (n = 4).

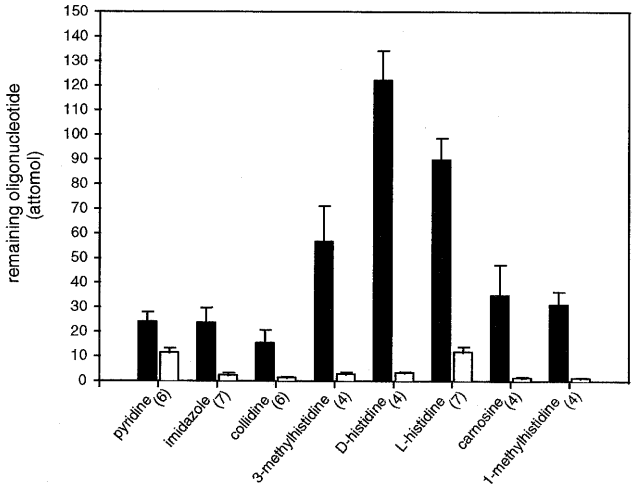

Figure 4. Low ionic strength buffers supporting specific hybridization. Using the buffers listed in Table 1, btrRCA5, 10 nM, was targeted using constant current (500 nA) to microelectrode sites at which either ATA5 or ATA4 had previously been anchored. Following transport, the arrays were washed with transport buffer and the residual fluorescent signal quantified, as described in Materials and Methods. Shown are results from those buffers that supported significantly increased oligonucleotide retention at the site of complementary capture oligonucleotide (ATA5) as compared with non-complementary oligonucleotide (ATA4). Solid bars, ATA5; open bars, ATA4. The number of pairwise comparisons is indicated by parentheses following each buffer. Data are presented as mean ± SEM.

non-linear behavior with increasing current. The rate of signal accumulation appears to reach a plateau as applied current is increased. This effect is more dramatic for histidine, a buffer with higher conductivity than GABA. The non-linear accumulation rates are again consistent with a more rapid build-up of ionic constituents or breakdown products of the buffer at higher currents.

Effect of electronic field application on hybridization

The effect of electronic concentration of oligonucleotides on hybridization rate is shown in Figure 3. In this experiment, an oligonucleotide was first electronically directed to and then anchored at selected sites of the microarray. The corresponding fluorescent labeled complementary oligonucleotide was introduced in either a high salt buffer (5× SSC), and allowed to passively hybridize (filled circles and squares), or was introduced in 50 mM histidine and electronically targeted to the capture oligonucleotide (open circles and squares). As shown, the electronically targeted oligonucleotide hybridization rate was 30- to 40-fold greater than the passive hybridization rate. No hybridization was observed using histidine in the absence of an applied electric field, irrespective of the time allowed (filled triangles). Thus, concentration alone may not fully explain the marked increase in efficiency of oligonucleotide hybridization in the electric field.

Despite rapid transport and high level accumulation of signal at the anodes, neither GABA, β-alanine, nor glycine was capable of supporting sequence-specific hybridization. Cysteine was difficult to evaluate because of poor signal accumulation. In contrast, other buffers such as histidine demonstrated specific hybridization (Fig. 4). In this figure, the ratio of complementary capture signal levels to non-complementary capture signal levels serves as an indicator of specificity (complementary > non-complementary, $P < 0.05$). These include histidine, substituted histidines, and heterocyclic species such as imidazole, pyridine and collidine (a trimethylated pyridine) (Fig. 5). A consistent feature of these buffers (listed in Table 2) is the presence of a weak base, e.g., imidazole ring, whose pKa value is near neutrality. In contrast, buffers which did not support hybridization contain no such buffering group. The failure of zwitterionic buffers such as GABA to support electronic hybridization, despite high accumulation, again suggests that factors other than oligonucleotide concentration are important. These results suggest that buffering capability at neutral pH is an important property for supporting hybridization under these conditions.

Further analysis of Table 2 reveals marked differences in the relative efficiencies of hybridization. That is, two distinct groupings appear in the data. One grouping consists of imidazole, pyridine and collidine. These compounds yielded an ~5-fold lower hybridization efficiency when compared with the other buffers, D- and L-histidine, carnosine and the methylated histidine derivatives. (These experiments were designed to reveal differences in hybridization efficiencies and, therefore, were performed under conditions that would not saturate available capture sites.) The more efficient buffers all contain an imidazole or substituted imidazole ring, yet are more efficient than imidazole alone in supporting hybridization. This suggests that other functional groups also aid in the hybridization process.

A final aspect of the data listed in Table 2 is the relatively poor hybridization efficiency of L-histidine as compared to other histidine-like compounds. Since specific hybridization is based upon subtracting the non-specific signal from the specific signal, then either of these parameters may influence the final hybridization efficiency. Evaluation of non-specific signal levels

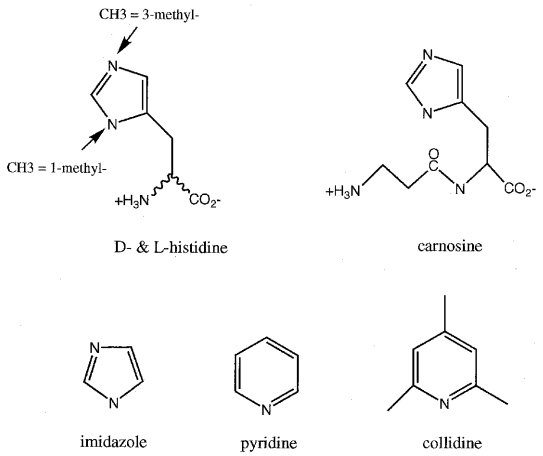

Figure 5. Chemical structure of buffers supporting hybridization.

compared to the amount of material transported indicates that L-histidine had a higher level of non-specific signal, 2.2%, as compared with the other histidine-like buffers, which were 1% or less. The reason for this higher retention in L-histidine is unclear, however other experiments indicate that this background signal can be removed with more extensive washing. It may be that the slightly higher transport in L-histidine as compared with the other histidine derivatives results in some threshold concentration such that more fluorescent oligonucleotide concentrates further within the permeation layer and is therefore more difficult to remove. Results from pyridine somewhat support this possibility. When compared with imidazole and collidine, pyridine has the highest transport and non-specific signal but, within its group, it also has the lowest efficiency of hybridization. However, differing non-specific interactions between L-histidine, oligonucleotide and, possibly, the permeation layer cannot be ruled out.

Table 2. Buffer hybridization efficiency

Buffer	Transported[a,b] (attomol)	Specific hybridization[a] (attomol)	Hybridization efficiency[c]
pyridine	764 ± 66	12.8 ± 4.2	1.7
imidazole	528 ± 63	21.2 ± 6.6	4.0
collidine	382 ± 63	14.1 ± 4.6	3.7
3-methylhistidine	259 ± 48	54.0 ± 14.8	20.8
D-histidine	490 ± 50	119 ± 11.8	24.3
L-histidine	533 ± 65	78.0 ± 9.1	14.6
carnosine	129 ± 45	33.7 ± 12.1	26.1
1-methylhistidine	141 ± 20	30.0 ± 5.0	21.3

[a]Data are presented as value ± SEM.
[b]Fluorescent signal present at completion of electronic targeting.
[c]Efficiency = [(specific hybridization)/(transported)] × 100.

Effect of pH on hybridization

As noted above, those buffers that successfully supported hybridization have titratable substituents with pKa values which are at or near neutral pH. This could be particularly important since acid is generated by electrolysis over the anode (capture site) during transport. To evaluate the effect of pH on hybridization, a micro-pH electrode, approximately 75 µm in outside diameter, was positioned at a constant distance just above the surface of the permeation layer over individual electrode sites. Since the hydrolysis of water generates protons at the electrode (or within the electrochemical double layer), a proton gradient extends from the electrode surface through the permeation layer and out into the solution. Therefore, pH measurements shown in Figure 6 may be somewhat higher than those experienced by the oligonucleotides which are anchored in the topmost portion of the permeation layer. In the absence of buffer, a dramatic decrease in the pH was observed even at low current levels, 200 nA (Fig. 6A). At 500 nA, the unbuffered system demonstrated an extremely rapid drop in pH (Fig. 6B) and generated gas bubbles. In contrast, GABA was somewhat more effective in buffering the pH at low currents. Histidine and imidazole proved to be much more effective buffers maintaining the pH over the surface of the permeation layer above pH 5 for currents of either 200 or 500 nA.

These findings suggest that the imidazole ring may serve as the primary source of buffering for histidine and imidazole within this pH range. In contrast, GABA does not possess such a group and must therefore rely upon the carboxylate group for buffering at low pHs. These low pHs may not support hybridization of oligonucleotides well (17). Alternatively, inability to become protonated near neutral pH may prevent these buffers from providing cations that shield repulsion between the negatively charged phosphate backbones.

In order to clarify whether the inability of GABA to support hybridization is the result of either the acidic environment or by a failure to provide adequate cationic shielding, a neutral backbone (PNA) was substituted for the negatively charged phosphodiester backbone of the capture oligonucleotide and the effect of this substitution examined. Hybridization of PNA hybrids has been demonstrated to occur with similar affinities, but to be largely salt independent (18). A representative set of results from four sets of experiments examining the effect of PNA substitution is shown in Figure 7. This figure shows a comparison of the hybridization efficiency in histidine as compared to GABA using either PNA (solid bars) or DNA (clear bars) capture oligonucleotides and a common, fluorescent labeled DNA oligonucleotide. Hybridization in GABA was seen between the uncharged PNA backboned oligonucleotide and the DNA reporter oligonucleotide at 200 nA, whereas no hybridization was observed in the corresponding DNA:DNA pairing. Since similar degrees of local nucleotide concentration were achieved, this suggests that shielding of the phosphodiester backbone is an important component of the electronic hybridization process. This observation is further supported by the comparable pH values obtained in GABA at 200 nA and histidine at 500 nA (Fig. 6). No hybridization was observed in GABA at 200 nA despite a range of pH compatible with DNA:DNA hybridization. Therefore, some component other than pH appears to be required for hybridization.

However, if the pH is reduced below a critical level, the acidity will be too great to support hybridization between the nucleotide

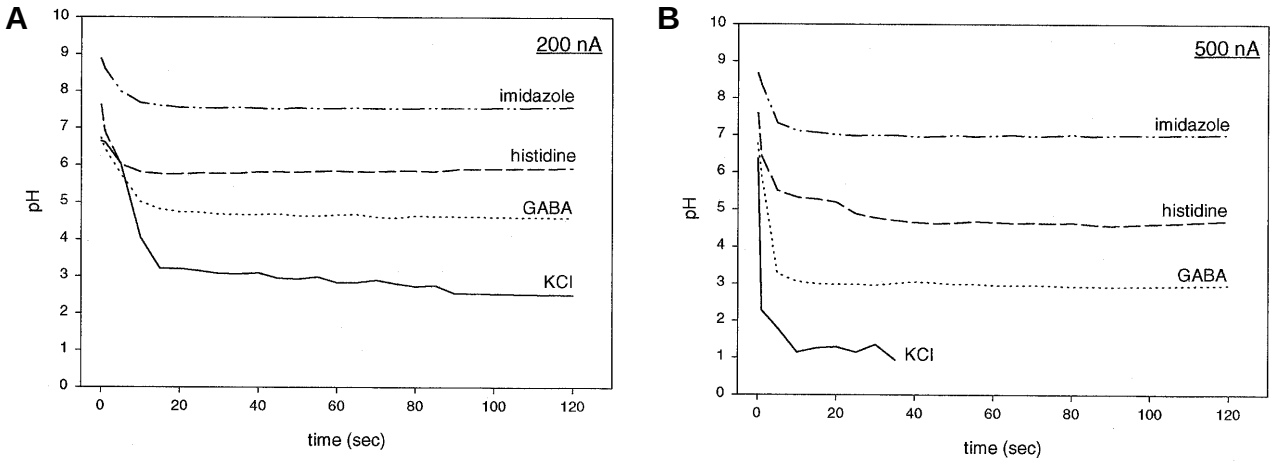

Figure 6. Effect of different currents and buffers upon pH. Using an antimony microelectrode, pH values above the surface of individual microelectrodes of an agarose coated APEX array were measured in either 50 mM imidazole, 50 mM L-histidine, 50 mM GABA or 50 mM KCl, as described in Materials and Methods. Individual microarray electrodes served as anodes during the application of either 200 nA (**A**) or 500 nA (**B**) over the times indicated.

bases. This may account for the lack of hybridization with either PNA:DNA or DNA:DNA duplexes at 500 nA in GABA.

In contrast, DNA:DNA hybridization in histidine only occurs well at 500 nA (clear bar), while PNA:DNA hybridization occurs at roughly equal efficiencies at either current (solid bars). These currents correspond to higher pH values in histidine than in GABA. At 200 nA, the pH of the solution is ≈6 whereas, at 500 nA, the pH is ≈5. Therefore, at 200 nA, fewer histidine molecules have protonated imidazole rings when compared with 500 nA. A higher concentration of protonated species may be suitable for shielding phosphodiester backbones and permitting hybridization of DNA.

To test whether protonation of histidine aids hybridization, passive (non-electronic) hybridization was performed. As shown in Figure 8, histidine at its pI (pH 7.5) does not facilitate hybridization. At this pH, few histidine molecules will possess a net positive charge for any significant time. In contrast, histidine at pH 6.0 and 5.0 accelerated hybridization. Thus, there appears to be a correlation between the ability of histidine to support hybridization and its degree of protonation. That shielding could be more effective is demonstrated by the greater effectiveness of SSC which contains nearly 1 M salt as compared with the 50 mM histidine. However, as the solution became more acidic, hybridization in histidine decreased. This was probably due to effects upon the oligonucleotides themselves and not attributable to increased protonation of histidine, which would increase the net positive charge on histidine and aid hybridization. Taken together with the

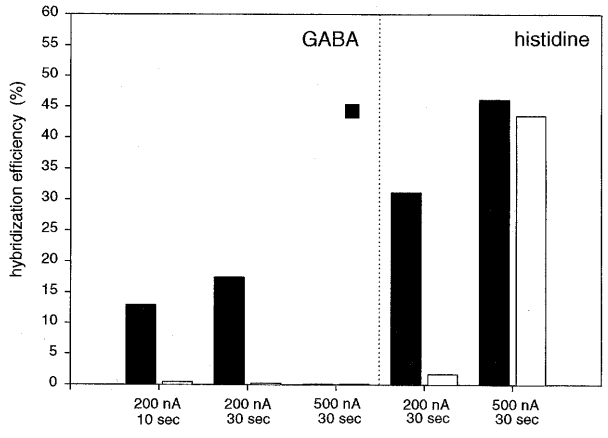

Figure 7. Comparison of hybridization efficiencies using phosphodiester-linked oligonucleotides and PNA-linked oligonucleotides. Either phosphodiester-linked oligonucleotides, or the corresponding PNA-linked oligonucleotides were microdeposited at individual sites upon the microarray. An oligonucleotide labeled with a fluorescent tag was added in either 50 mM L-histidine or 50 mM GABA and then targeted to individual sites upon the array using constant current, 500 nA, for the indicated time periods. Hybridization efficiency was calculated as described in Materials and Methods. Solid bars, PNA:DNA specific hybridization; open bars, DNA:DNA specific hybridization.

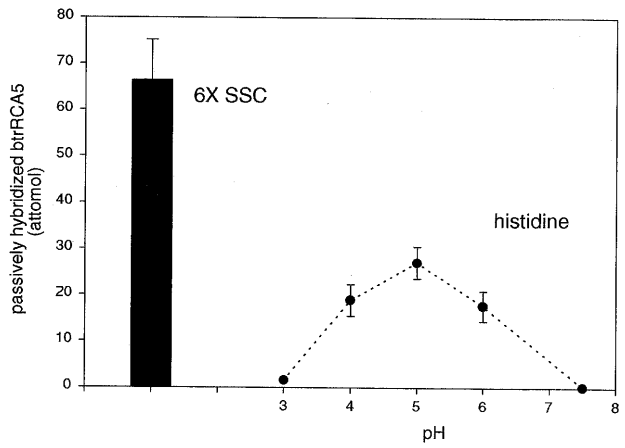

Figure 8. Effect of pH upon passive hybridization efficiency in histidine. As noted in Materials and Methods, 100 nM btrRCA5 was incubated for 15 min in 50 mM L-histidine adjusted to the indicated pH values (●) or in 6× SSC (vertical bar) on microarrays containing previously anchored ATA5 or ATA4. The chips were washed and the remaining fluorescence quantified at each site. Specific hybridization was calculated as complementary signal minus non-complementary signal. Data are presented as mean ± SD (n = 10).

previous results, it therefore appears that a combination of factors including concentration, maintenance of the pH near neutrality and the generation of a cationic species suitable for shielding the nucleotide phosphodiester backbones all contribute to electronically mediated hybridization of DNA:DNA complexes under these conditions.

DISCUSSION

The application of electric fields to microscale oligonucleotide arrays allows great acceleration and exquisite control over hybridization reactions. These advantages are augmented by the use of low conductivity or certain zwitterionic buffers. In general, these low-ionic strength buffers allow efficient transport of oligonucleotides to discrete sites in the presence of an applied current. These buffers do not support passive hybridization and, therefore, electronic control permits hybridization only at programmed sites. In addition to the mass action effect of concentration, our results suggest that the electrochemically-mediated production of positively charged buffer ions also facilitates the hybridization process. We have noted that a select subgroup of low conductivity buffers support hybridization under these conditions. Thus, we can separate transport from hybridization through the buffers and currents employed.

This programmed pH gradient allows discrete activation of hybridization zones and is a novel application for microelectronic devices. In our case, the buffering serves two roles: (i) it maintains the pH as close to neutrality as possible; and (ii) it actively participates in the reaction. In fact, if the pH is lowered below a critical threshold value, hybridization will be hindered. In short, in alleviating the detrimental pH effects created by hydrolysis at the anode, a species beneficial to the hybridization reaction is generated.

Interestingly, the efficiency by which these buffers support the hybridization process appears dependent upon the nature of the functional groups present. That is, once the criteria for possessing a buffering capacity within the hybridization window and the resultant generation of a positively charged species have been met, other functional groups may influence the hybridization process. The 5-fold increase in efficiency for histidine and related molecules over imidazole alone may reflect histidine's ability to sustain a positive charge on both the imidazole ring as well as the primary amine. Like simple dicationic salts such as Mg^{++}, this double positive charge may be more efficient at diminishing backbone repulsion. Further modification of these zwitterions may lead to additional increases in hybridization efficiency.

The utility of these microelectronic devices is just beginning to be explored. As a group, they utilize lower quantities of reagents and often have significantly greater sensitivity and speed than conventional procedures. Ultimately, they may allow replacement of our present macro-scale molecular biology equipment by suitable microscopic devices.

ACKNOWLEDGEMENTS

The authors gratefully acknowledge the intellectual contributions and support of Drs Tina S. Nova and James P. O'Connell throughout the course of this work and for helpful insight into electrochemical processes by Eve Fabrizio.

REFERENCES

1 Chee, M., Yang, R., Hubbell, E., Berno, A., Huang, X.C., Stern, D., Winkler, J., Lockhart, D.J., Morris, M.S. and Fodor, S.P.A. (1996) *Science* **274**, 610–614.
2 Lockhart, D.J., Dong, H., Byrne, M.C., Follettie, M.T., Gallo, M.V., Chee, M.S., Mittman, M., Wang, C., Kobayashi, M., Horton, H. and Brown, E.L. (1996) *Nature Biotechnol.* **14**, 1675–1680.
3 Weiler, J. and Hoheisel, J.D. (1996) *Anal. Biochem.* **243**, 218–227.
4 Eggers, M. and Ehrlich, D. (1995) *Hematologic Pathol.* **9**, 1–15.
5 Ferguson, J.A., Boles, T.C., Adams, C.P. and Walt, D.R. (1996) *Nature Biotechnol.* **14**, 1681–1684.
6 Schena, M., Shalon, D., Davis, R.W. and Brown, P.O. (1995) *Science* **270**, 467–470.
7 Heller, M.J. (1996) *IEEE Engng Med. Biol.* **15**, 100–103.
8 Sosnowski, R.G., Tu, E., Butler, W.F., O'Connell, J.P. and Heller, M.J. (1997) *Proc. Natl. Acad. Sci. USA* **94**, 1119–1123.
9 Ausubel, F.M., Brent, R., Kingston, R.E., Moore, D.D., Seidman, J.G., Smith, J.A. and Struhl, K. (1994) *Current Protocols in Molecular Biology*. John Wiley & Sons, NY, USA.
10 Horrocks, B.R., Mirkin, M.V., Pierce, D.T., Bard, A.J., Nagy, G. and Toth, K. (1993) *Anal. Chem.* **65**, 1213–1224.
11 Bicher, H.I. and Ohki, S. (1972) *Biochim. Biophys. Acta* **255**, 900–904.
12 Matsumara, Y., Kajino, K. and Fujimoto, M. (1980) *Membrane Biochem.* **3**, 99–129.
13 Glab, S., Hulanicki, A., Edwall, G. and Ingman, F. (1989) *Crit. Rev. Anal. Chem*. **21**, 29–47.
14 Davis, D.G. and Bianco, E. (1966) *J. Electroanal. Chem.* **12**, 254–260.
15 Oldham, K.B. (1988) *J. Electroanal. Chem.* **250**, 1–21.
16 Newman, J.S. (1991) *Electrochemical Systems*, Prentice Hall, Englewood Cliffs, NJ, chapter 11.
17 Bloomfield, V.A., Crothers, D.M. and Tinoco, I. (1974) *Physical Chemistry of Nucleic Acids*. Harper and Row, New York, NY.
18 Egholm, M., Buchardt, O., Christensen, L., Behrens, C., Freier, S.M., Driver, D.A., Berg, R.H., Kim, S.K., Norden, B. and Nielsen, P.E. (1993) *Nature* **365**, 566–568.